

Doppler Profiles of Radio Frequency Interference

B. K. Levitt

Communications Systems Research Section

The DSN is currently developing a wideband, digital system for monitoring the RF environment at each receive complex. One of the characteristics that will be used to identify observed RFI (radio frequency interference) sources is the time variations of their received spectra. As a preliminary aid to this effort, doppler profiles were computed for Earth satellites and planes with typical flight parameters. The analysis shows that doppler rates will be high enough to cause spectral smearing and degrade the surveillance station detection capability under certain conditions.

I. Introduction

The DSN is in the process of developing a wideband, digital surveillance system for on-site detection and identification of radio frequency interference (RFI) sources (Reference 1). When a signal of interest is detected, its identity will be determined on the basis of any or all of the following observations: time and duration of occurrence, source direction, polarization, spectral characteristics and their time variations, and a comparison of these data with previously identified RF signatures in storage. Focussing on the spectral variation aspect, doppler profiles were computed for Earth satellites and planes over a range of expected flight parameters, as a preliminary aid to the identification effort.

$$v = \frac{631.3}{\sqrt{r}} \quad (1)$$

Assume further that the satellite passes directly over the RF surveillance station, and that it is transmitting at S-band (center frequency $f_0 \cong 2295$ MHz). Also, neglect the Earth's rotation (a second-order effect) and use $r_0 = 6357$ km for the Earth's radius.

Referring to Fig. 1, the satellite-to-surveillance station range s is given by

$$\begin{aligned} s^2 &= r^2 \sin^2 \theta + (r \cos \theta - r_0)^2 \\ &= r^2 (1 + \gamma^2 - 2\gamma \cos \theta); \quad \gamma \equiv r_0/r \end{aligned} \quad (2)$$

$$\begin{aligned} &\Downarrow \\ 2s \frac{ds}{dt} &= 2r^2 \gamma \sin \theta \frac{d\theta}{dt} \end{aligned} \quad (3)$$

II. Earth Satellites

To facilitate the doppler calculations, assume the satellite is in a circular orbit, with radius r (km), tangential velocity v (km/s), and constant angular velocity $d\theta/dt = v/r$ (rad/s). Equating gravitational and centrifugal forces on the satellite yields the relation (Reference 2)

The satellite signals received at the surveillance station exhibit a doppler shift

$$f = -\frac{f_0}{c} \left(\frac{ds}{dt} \right) = -\frac{f_0 v \gamma \sin \theta}{c \sqrt{1 + \gamma^2 - 2\gamma \cos \theta}}; |\theta| \leq \theta_0 \quad (4)$$

where $\theta_0 = \cos^{-1} \gamma$, and $c = 3 \times 10^5$ km/s is the velocity of light. The maximum doppler shift occurs at $\theta = \pm \theta_0$:

$$|f|_{\max} = \frac{f_0 v \gamma}{c} \propto r^{-3/2} \quad (5)$$

The doppler rate for the received satellite signals is given by

$$\frac{df}{dt} = -\frac{f_0 v^2 \gamma}{c r \sqrt{1 + \gamma^2 - 2\gamma \cos \theta}} \left(\cos \theta - \frac{\gamma \sin^2 \theta}{1 + \gamma^2 - 2\gamma \cos \theta} \right) \quad (6)$$

The maximum doppler rate occurs at $\theta = 0$:

$$\left| \frac{df}{dt} \right|_{\max} = \frac{f_0 v^2 \gamma}{c r (1 - \gamma)} \quad (7)$$

Note that $df/dt = 0$ at $\theta = \pm \theta_0$, so that the doppler shift reaches its maximum amplitude each time the satellite crosses the surveillance station horizon. The total observation time from horizon to horizon is

$$T = \frac{2 \theta_0}{d\theta/dt} = \frac{2r}{v} \cos^{-1} \gamma \quad (8)$$

Earth satellite altitudes typically range between 300 and 1200 km (Ref. 2); doppler parameters are tabulated below for altitudes in this range.

$r - r_0$ km	v km/s	$ f _{\max}$ KHz	$\left \frac{df}{dt} \right _{\max}$ KHz/s	T min
300	7.74	56.5	1.46	8.63
750	7.49	51.2	.512	14.7
1200	7.26	46.7	.283	19.8

Normalized doppler profiles for satellite signals are plotted in Fig. 2.

III. Planes

As shown in Fig. 3, the simplification here is that the plane is travelling in a straight line at a constant velocity v as it passes within range of the surveillance station. The plane-to-surveillance station range s at closest approach is s_0 : it need not be assumed that the plane is directly over the station at $s = s_0$. Letting time $t = 0$ at closest approach, the instantaneous range satisfies the relation

$$s^2 = s_0^2 + v^2 t^2 \quad (9)$$



$$2s \frac{ds}{dt} = 2v^2 t \quad (10)$$

The received doppler shift can be written in the form

$$f = -\frac{f_0 v \mu(t)}{c \sqrt{1 + \mu^2(t)}}; \mu(t) \equiv \frac{vt}{s_0} \quad (11)$$



$$|f|_{\max} = \frac{f_0 v}{c} \quad (12)$$

The doppler profile represented by Equations 11 and 12 is plotted in normalized form in Figure 4.

The doppler rate is given by

$$\frac{df}{dt} = -\frac{f_0 v^2}{c s_0} [1 + \mu^2(t)]^{-3/2} \quad (13)$$

$$\left| \frac{df}{dt} \right|_{\max} = \frac{f_0 v^2}{c s_0} \quad (14)$$

We might reasonably assume that plane velocities lie in the range between .05 and 1.00 km/s (110 to 2200 mi/hr). Furthermore, since faster planes typically fly at higher altitudes, assume the following ranges of s_0 for a given v :

v		min s_0		max s_0	
km/s	mi/hr	km	ft	km	ft
.05	110	1	3300	3	9800
.25	560	3	9800	12	39,000
1.00	2200	10	33,000	25	82,000

Based on these flight parameter assumptions, for S-band signals ($f_0 \cong 2295$ MHz), the surveillance station would observe the following maximum doppler shifts and doppler rates:

v km/s	$ f _{\max}$ kHz	s_0 km	$\left \frac{df}{dt}\right _{\max}$ KHz/s
.05	.38	1	.0190
		3	.0064
.25	1.9	3	.160
		12	.040
1.00	7.7	10	.77
		25	.31

IV. Conclusions

In the evolution of the digital RFI surveillance system design since Reference 1 was written, the current plan is to demonstrate a first-generation device at Goldstone in mid-1978, with the following features:

- 15 dB gain, 30° beamwidth, circular horn antenna with low, fixed elevation direction, rotating 360° in azimuth every minute

- generation of a 20 MHz spectrum, containing 2^{16} or about 65,000 lines (305 Hz resolution), every 5 seconds

Thus, an RF source in a given azimuthal direction will be observed for 5 seconds of each minute it is within range of the surveillance station.

Based on the assumptions in the previous two sections, upper and lower bounds for satellite and plane doppler profiles are compared in Figure 5. It is evident that the observed doppler signatures will be very useful for identifying mobile RF sources and their trajectories. Also, because the doppler rate is often very large near closest approach, there will be some spectral smearing in this region: obviously, this effect is more critical for line spectra than for wideband signals. This smearing effect can impact the RF detection capability: for example, a CW signal that barely exceeds the surveillance system threshold under zero doppler rate conditions will not be detected if the doppler rate is too high. As a benchmark, the 61 Hz/s doppler rate point is shown in the doppler profiles of Figure 5 (the doppler rate is always less than this level for the $v = .05$ km/s, $s_0 = 3$ km plane case): at this doppler rate, a CW spectral line will move through one resolution bin over the 5 second observation time.

References

1. Levitt, B. K., "Analysis of a Discrete Spectrum Analyzer for the Detection of Radio Frequency Interference," in *"The Deep Space Network Progress Report 42-38"*, Jet Propulsion Laboratory, Pasadena, California, pp. 83-98, April 15, 1977.
2. Levitt, B. K., "Radio Frequency Interference from Near-Earth Satellites," in *The Deep Space Network Progress Report 42-37*, Jet Propulsion Laboratory, Pasadena, California, pp. 69-77, February 15, 1977.

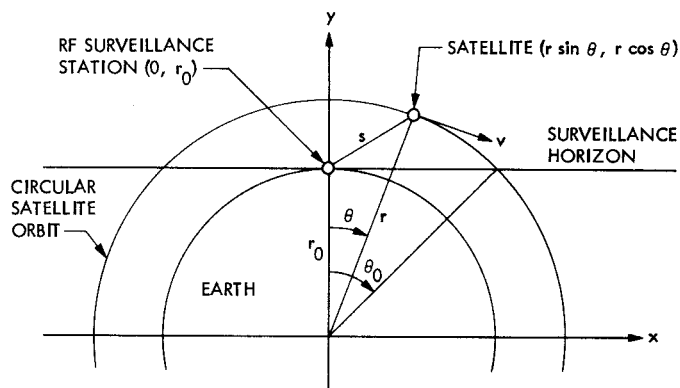


Fig. 1. Earth satellite doppler geometry

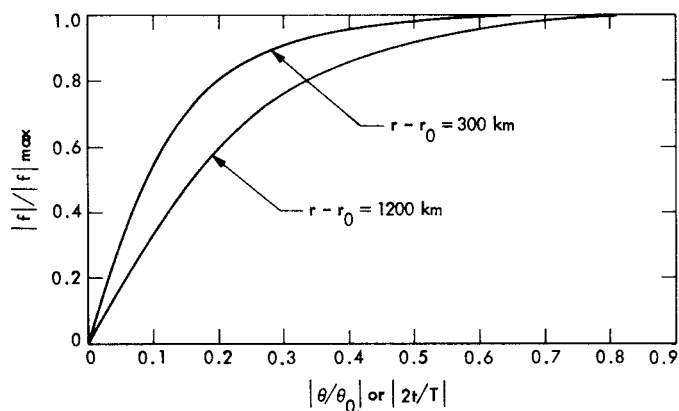


Fig. 2. Normalized doppler profiles for satellite signals received at a surveillance station. Zero-time reference ($t = 0$) is at closest approach ($\theta = 0$)

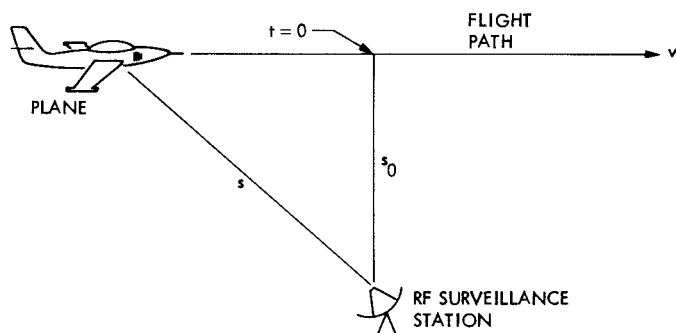


Fig. 3. Plane doppler geometry

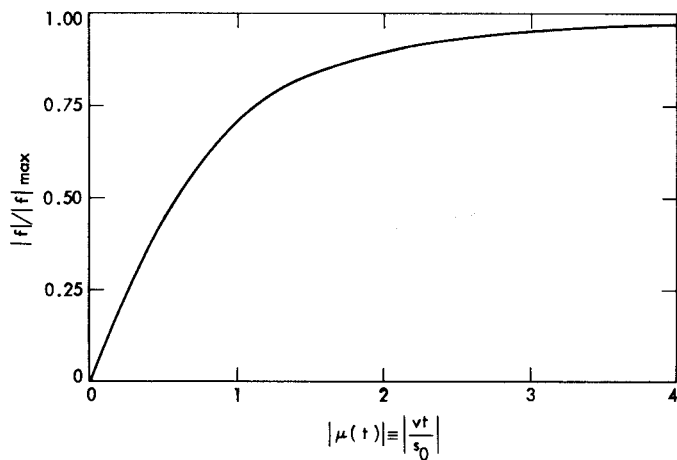


Fig. 4. Normalized doppler profile for plane. Time $t = 0$ at closest approach (range $s = s_0$)

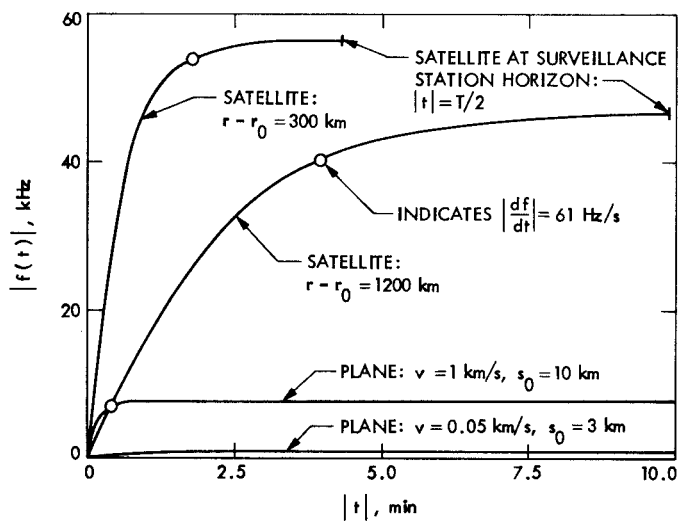


Fig. 5. Comparison of satellite and plane doppler profiles. (See text for explanation of symbols in this graph.)